



CE-MU-OFDM-PM Signal Design and Analysis for NavCom

Jing Ji^{1,2}, Wei Chen^{3(✉)}, Yuting Liu³, Luyao Du³, and Hongyang Lu^{1,4}

¹ School of Information Engineering, Wuhan University of Technology, Wuhan 430074, China

jijingisme@whut.edu.cn

² Wuhan Xingtu Electronics Co., Ltd, Wuhan 430074, China

³ School of Automation, Wuhan University of Technology, Wuhan 430074, China

greatchen@whut.edu.cn

⁴ Department of Navigation, CTTIC, Beijing 100011, China

Abstract. With the successive large-scale launches of low-earth orbit satellites (LEOs), satellite-based augmentation systems (SBAS) have become an important supplementary part of the GNSS system. However, the emergence of new concepts such as B5G/6G, national integrated positioning, navigation and timing systems (PNTs), has brought new challenges to the integration of navigation and communication (NavCom), but the core issue is still the challenge of the signal system. This paper proposes a new signal scheme. Through preliminary research on the same frequency band or adjacent frequency bands, it is found that this scheme is more suitable for S-band and has a wider normalized power spectral density (PSD) and peak sidelobe ratio (PSR). And the multi-peak characteristics of autocorrelation. Through the analysis of simulation performance evaluation, it is found that the proposed scheme has high potential positioning accuracy. The code tracking accuracy can reach 0.85 m and the carrier-to-noise ratio (CNR) is 20 dB-Hz. The proposed signal has less mutual influence with other candidate signals, and has better anti-multipath ability. At the same time, it is in terms of code tracking anti-matching spectrum interference factor, demodulation anti-matching spectrum interference factor, and demodulation anti-narrowband interference factor, the proposed signal also has excellent performance. Therefore, from the perspective of technical feasibility and theoretical evaluation, the signal proposed in this paper is superior to other candidate signals. And from an application point of view, the solution we propose can be used as a competitive potential signal solution for BDS in the future, and it is also B5G/6G foundation and PNT.

Keywords: Signal design · LEOs · NavCom · BDS · PNTs · CE-MU-OFDM-PM

1 Introduction

Global Navigation Positioning System (GNSS), as a crucial spatial-temporal infrastructure, provides position, velocity and time (PVT) services for all kinds of users

© Aerospace Information Research Institute 2022

C. Yang and J. Xie (Eds.): *China Satellite Navigation Conference (CSNC 2022) Proceedings*, LNEE 910, pp. 417–432, 2022.

https://doi.org/10.1007/978-981-19-2576-4_37

around the world. In 2020, BeiDou phase 3 has been launched and completed, becoming the third system that provides global PVT services after GPS and GLONASS [1]. However, due to the fragility of the GNSS system itself, the service cannot meet all users' requirements, especially the indicators of accuracy, availability, integrity, and anti-interference etc., it limits the application of GNSS.

To meeting the requirement of differentiated users, positioning, navigation, timing and communication (PNTC) capabilities have been extended to a wider range of fields. This term was formally proposed by Prof. Liu Jingnan [2, 3], and this concept was also the positive response by Prof. Yang Yuanxi, Prof. Li Deren, etc. scholars [4–6]. At the same time, integration of navigation and communication (NavCom) is also being widely used at the signal level. Prof. Deng Zhongliang, Beijing University of Posts and Telecommunications proposed an integrated indoor and outdoor conduction signal fusion based on the TC-OFDM carrier signal modulation system. Through testing and evaluation, the accuracy of the signal can reach the meter level [7]. Prof. Liu Xiaoli of Wuhan University proposed a carrier signal modulation system based on MSK and OFDM. At the same time, the two signals were evaluated through the navigation contribution and tracking performance. The above two signals are considered to be better than the other signals studied in the paper. Have better performance [8]. PhD Luo Ruidan and Prof. Xu Ying proposed a multi-carrier composite navigation signal modulation method. Compared with the existed candidate modulation signal, it has better tracking accuracy, anti-interference and spectrum utilization performance, and it can be used as a navigation enhancement system signal [9].

As one of the authorized GNSS navigation bands, S-band with 16.5 MHz bandwidth becomes more precious with the shortage of authorized spectrum resources. At the same time, compared with the traditional L-band, it has time convergence, rain attenuation, ionospheric delay, and antenna size. It has more advantages in terms of antenna gain. At the same time, as the software defined radio (SDR) be fully applied on the satellite payload and receiver, the traditional transceiver cost problem can be almost ignored. In addition, this band couples; multiple systems and services, to provides an opportunity for the NavCom on the signal level. All above factors make us pay more attention to the signal design with S-band potential.

Galileo system has paid great attention to it in the early stage, even established a candidate modulation signal pool. For a series of candidate carrier modulation signals including BOCs(5,2) and BPSK(1). It has been verified the performance indicators of the candidates on the ground at the signal level. At the same time, the indicators of the candidates are actually verified at the system level, and a test verification satellite is even launched for this purpose [10–12]. Scholars such as Prof. Xue Rui and Prof. Yanbo Sun proposed the use of a continuous phase modulation (CPM) scheme in the S-band, and verified that it has outstanding code tracking accuracy, anti-interference ability and multipath cancellation ability [13]. Wang Lei proposed a spread spectrum modulated signal based on MSK, and found that SSMSK signal has better acquisition, tracking and user capacity through performance evaluation [14].

The organization of this paper is as follows: the 1st section introduces GNSS development and current status of the S-band carrier signal research. The 2nd investigates the

existing related systems and services in target band. The 3rd section proposed mathematics model, signal generating flowchart, and basic analysis. The 4th section evaluates the code tracking, compatibility, anti-multipath, anti-jamming and communication payload. Finally, summarizes and prospects.

2 Target Band Survey

The main influence factors on the signal scheme design of the target band are co-band jamming and adjacent-band jamming. At present, the primary systems and services coexisted in- and adjacent-band as listed (see Table 1), and the primary signal of services (see Fig. 1).

There are a large number of signal sources are distributed throughout the land, sea, air and space, including GEO/MEO/LEO constellations, LTE 4G/5G, territorial base-stations and near-field communication, all above sources emit radio waves uninterrupted, at the same time, radio-receivers are detected, acquired, and tracked these radios, to provide users with position, navigation, timing and communication services.

According to the ITU regional frequency service division, RDSS is the main service in the Americas, but it is a secondary service in Europe, Africa, the Middle East, North Asia and the Asia-Pacific region. In addition, ITU-R is protecting the main services and supporting the services integration of RDSS/MSS. IRNSS, a regional navigation system, with a carrier center of 2492.028 MHz, and is modulated by BPSK(1) and BOC(5,2) respectively to provide standard positioning service (SPS) and Restrict Service (RS) service. The minimum received power of SPS reach -162.3 dBW. Globalstar, a global satellite system, is consisting of 48 LEO constellations. It will continue to provide mobile voice and data communication services before 2025. It uses frequency multiplexing technology to divide the 16.5 MHz bandwidth into 13 sub-beams to effectively avoid aliasing, each sub-beam has a bandwidth of 1.23 MHz [15, 16].

Table 1. The primary systems of in-band/adjacent- for s-band.

| Types | Systems | Frequency band consistency | Bandwidth | Modulation |
|--------------------|----------------|----------------------------|-----------|----------------------|
| Satellite source | BDS-RDSS | ✓ | 16.5 MHz | BPSK(4) |
| | IRNSS | ✓ | 16.5 MHz | BPSK(1) BOCs(5,2) |
| | Globalstar | ✓ | 16.5 MHz | SRC(0.2,1) |
| Territorial source | TD-LTE Band-41 | 2496–2690 | 20 | QPSK/OFDM |
| | TD-LTE Band-53 | Sub frequency | 11.5 | QPSK/OFDM |

(continued)

Table 1. (continued)

| Types | Systems | Frequency band consistency | Bandwidth | Modulation |
|-----------|------------------------------------|----------------------------|-----------|-----------------|
| | WiMAX | 2496–2690 | 1.75–20 | OFDM |
| | Wi-Fi the 14 th channel | 2473–2495 | 22 | DSSS/OFDM |
| | FS | 2450–2690 | / | MSK/QPSK |
| Candidate | Galileo | ✓ | / | Chirped BPSK(1) |
| | BDS | ✓ | / | CBOC(6,1,1/11) |

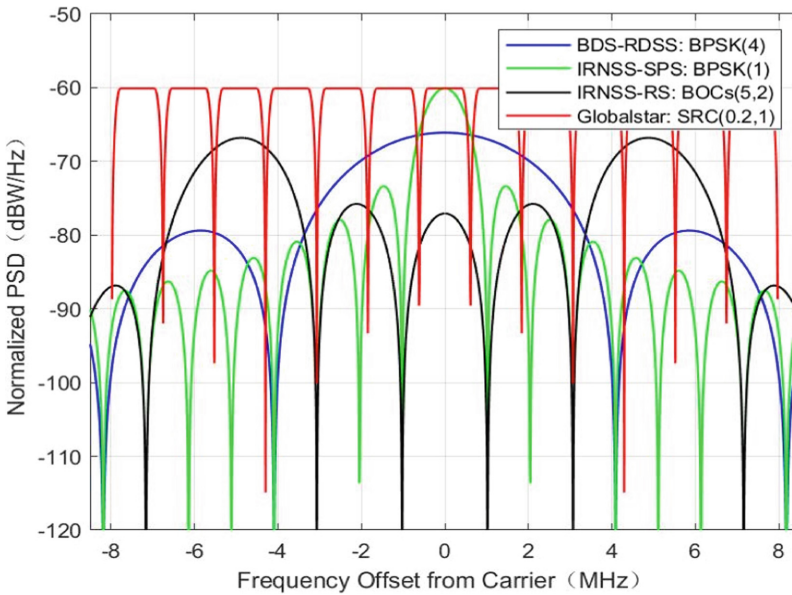


Fig. 1. The normalized PSD function of the primary services.

3 Model

3.1 Signal Model

The carrier signal modulation scheme proposed in this paper is named Multi-User Orthogonal Frequency Division Multiplexing Continuous Phase Constant Envelope Modulation (CE-MU-OFDM-PM).

The CE-MU-OFDM-PM time-domain mathematical model is defined as,

$$s(t) = A \cdot \text{Re}\{ \exp[j\phi(t)] \} \tag{1}$$

where A denotes signal amplitude, $\text{Re}\{\cdot\}$ and $\phi(t)$ represents real operator and time-varying phase function, respectively. Variable can be expressed as,

$$\phi(t) = \theta_i + 2\pi h C_N \sum_{k=1}^N I_{i,k} q_k(t - iT_c) \quad (2)$$

and $iT_c \leq t \leq (i+1)T_c$, our signal generating model as shown (see Fig. 2).

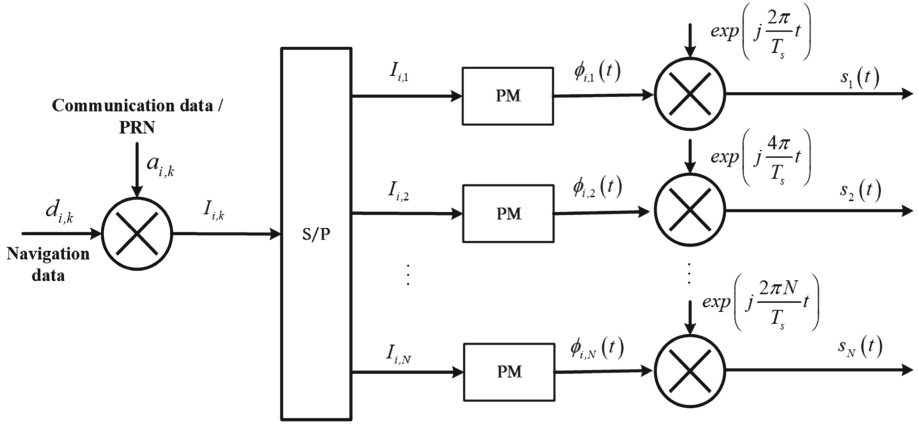


Fig. 2. Proposed signal generating model.

In Eq. (2), θ_i is the phase of the i -th symbol. Among them, h is the phase modulation factor, C_N is the normalization constant, $I_{i,k}$ is the i -th symbol, and the data symbol of the k -th subcarrier, $I_{i,k} = \pm 1$, T_c is the symbol period, $\{q_k(t)\}$ denotes waveform shaping function of the k -th subcarrier.

The parallel data symbol can be expressed as,

$$I_{i,k} = a_{i,k} \cdot d_{i,k} \quad (3)$$

where $a_{i,k}$ are binary pseudo-random numbers $\{0, 1\}$, and $d_{i,k}$ are binary navigation data $\{0, 1\}$. The sub-carrier orthogonal constraint as,

$$\int_{iT_c}^{(i+1)T_c} q_{k_1}(t - iT_c) \cdot q_{k_2}(t - iT_c) dt = \begin{cases} T_c/2, & k_1 = k_2 \\ 0, & k_1 \neq k_2 \end{cases} \quad (4)$$

The hypothesis is that the phases between various symbols meet the constraint of mutual independence, that is, the memory term in the phase is zero. At the time, the Eq. (1) can be expressed as,

$$s(t) = A e^{j\sigma_\phi p(t)} = A \sum_{n=0}^{\infty} \frac{(j\sigma_\phi)^n}{n!} p^n(t) \quad (5)$$

where σ_ϕ^2 denotes the signal phase D-value, $\sigma_\phi^2 = (2\pi h)^2$, and function $p(t)$ is the normalized orthogonal frequency division multiplexing (OFDM) signal modulation, it can be expressed as,

$$p(t) = C_N \sum_i \sum_{k=1}^N I_{i,k} q_k(t - iT_c) \tag{6}$$

3.2 Power Spectral Density and Autocorrelation Function

The normalized power spectral density (PSD) of our proposed signal scheme can be defined as,

$$G(f) = \frac{T_c}{2N} \sum_{k=1}^N \text{sinc}^2 \left[\left(f - \frac{k}{2T_c} \right) T_c \right] + \text{sinc}^2 \left[\left(f + \frac{k}{2T_c} \right) T_c \right] \tag{7}$$

where $\text{sinc}(\cdot)$ denotes the sampling function operator. It shows the normalized PSD function of proposed signal in different subcarriers k (see Fig. 3).

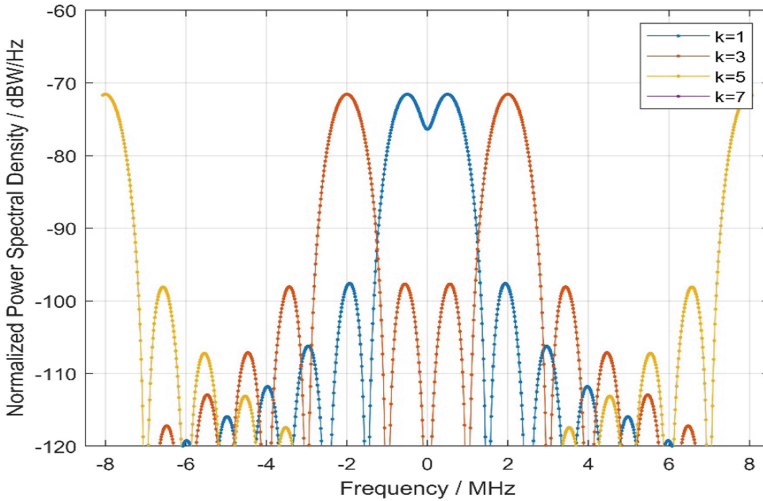


Fig. 3. The normalized PSD of the proposed signal

For different k , the normalized PSD function has characteristics as below:

- With the number of carriers increases, the PSD function increases the distance between the main lobes.
- The amplitude difference between the main lobe and the first side lobe in the normalized power spectral density function is 26.5 dBW/Hz.
- When $k = 1$, the main lobe bandwidth can reach 3.069 MHz, otherwise the main lobe bandwidth is 2.046 MHz, and all side lobe bandwidths are 1.023 MHz.

After inverse transformation, the autocorrelation function (ACF) of the CE-MU-OFDM-PM carrier signal scheme can be described as,

$$R(\tau) = \int_{-B_r/2}^{B_r/2} \frac{T_c}{2N} \sum_{k=1}^N \sin c^2 \left[\left(f - \frac{k}{2T_c} \right) T_c \right] + \sin c^2 \left[\left(f + \frac{k}{2T_c} \right) T_c \right] \cdot e^{j2\pi f \tau} df \quad (8)$$

where B_r denotes the front-end bandwidth of the receiver filter, it shows the ACF of the proposed signal (see Fig. 4).

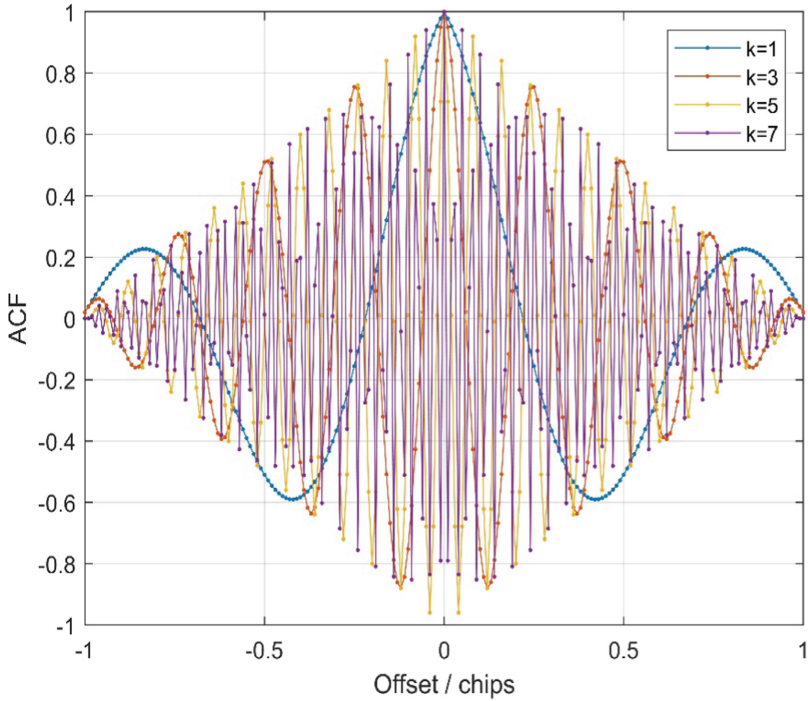


Fig. 4. The ACF of the proposed signal

It can be seen that the ACF of the proposed signal has characteristics as below,

- With the value of k increases, ACF has multiple peaks in a single cycle.
- With the value of k increases, the distance between ACF peaks is the same.
- For the same value with k , the interval between ACF peaks is the same.

The above-mentioned features can help the receiver to better acquire and track the signal when the parameters are known, and have outstanding resolution capabilities for multi-path.

4 Simulation, Result and Analysis

4.1 Simulation Test

The list of parameters used for NavCom simulation as shown (see Table 2).

Table 2. Simulation parameters.

| Indicators | Parameters |
|--|---------------------|
| Signal scheme | CE-MU-OFDM-PM |
| Frequency range | 2483.5 MHz–2500 MHz |
| Centre carrier frequency | 2491.75 MHz |
| Effective bandwidth | 16 MHz |
| Propagation distance | 500 km–1000 km |
| Uplink channel information rate | 64,000 bps |
| Downlink channel information rate | 4,096,000 bps |
| Satellite transmitter antenna gain | 20 dBi |
| Satellite transmitter power | 13 dBW |
| Receiver antenna gain | 11 dBi |
| Receiver power | 3 dBW |
| Systematic loss | 1 dB |
| Feeder noise coefficient | 0.8 |
| Satellite antenna equivalent noise temperature | 290 K |
| LNA equivalent noise temperature | 80 K |
| Satellite antenna equivalent noise temperature | 442.2 K |
| Receiver equivalent noise temperature | 250 K |

4.2 Navcom Performance Evaluation

This subsection will evaluate our carrier signal modulation scheme in accuracy, compatibility, anti-multipath, anti-jamming, spectrum multiplex and communication link payload as below.

Accuracy Potential

This paper uses code tracking error and Gabor bandwidth as assessment indicators in the accuracy potential for accuracy, and the simulation results are shown as Fig. 5 and Fig. 2, respectively.

In Fig. 5, it shows that the CE-MU-OFDM-PM marked by the red dotted line has excellent tracking accuracy only higher than the pulse-like SRC signal. However, when the carrier-to-noise ratio equals 15 dB-Hz, the code tracking accuracy can be reached about 1.2 m, it is significantly better than other candidate signals.

In Fig. 6, it shows that the Gabor bandwidth of various spread spectrum modulation signals, when the front-end bandwidth of the receiver is less than 14 MHz, the Gabor bandwidth of the proposed signal is very small, which means that it is not suitable for traditional economical narrowband receivers. When the front-end bandwidth exceeds 14 MHz, its gradient increases sharply. When the front-end bandwidth reaches about 16 MHz, it obtains a Gabor bandwidth equivalent to MSK (10), it shows that our signal scheme is very suitable for integration narrowband and wideband receivers.

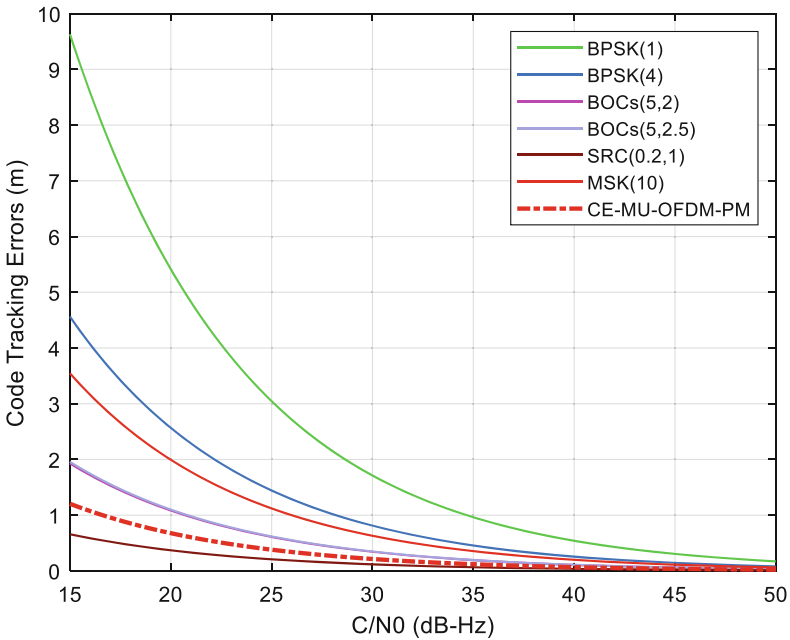


Fig. 5. Code tracking errors between proposed and others

Compatibility

This paper adopts the spectral separation coefficient (SSC) and the code tracking spectral sensitivity coefficient (CT-SSC) as assessment indicators for compatibility, the simulation results are shown as Fig. 7 and Fig. 8.

With SSC smaller, the easier it is to extract the target signal in mixed-signal. In Fig. 7, it shows that the SSC between our proposed signal and almost every type of candidate signal in the target frequency band is the smallest, it fully demonstrates that the proposed signal has better separation characteristics from existing or candidate signals.

With CT-SSC being smaller, the influence of the interference signal is mini more on the tracking performance of the target signal;s spread spectrum code. In Fig. 8, it

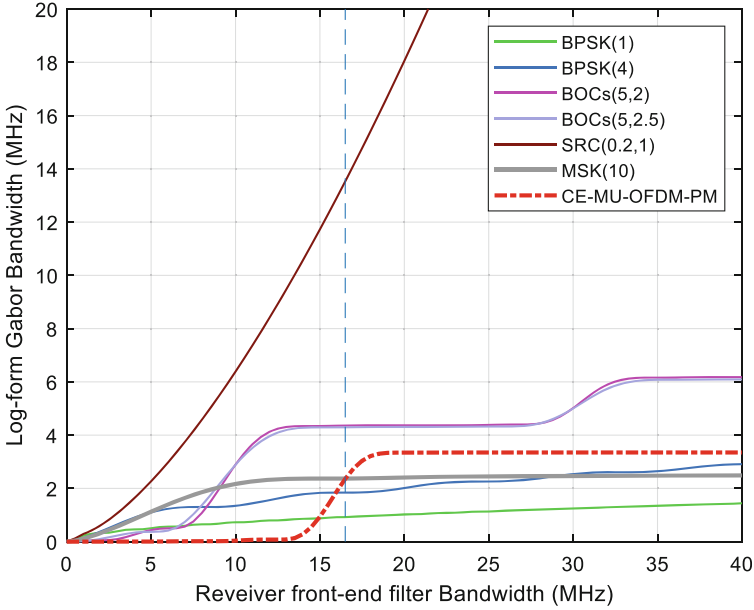


Fig. 6. Gabor bandwidth for proposed and others

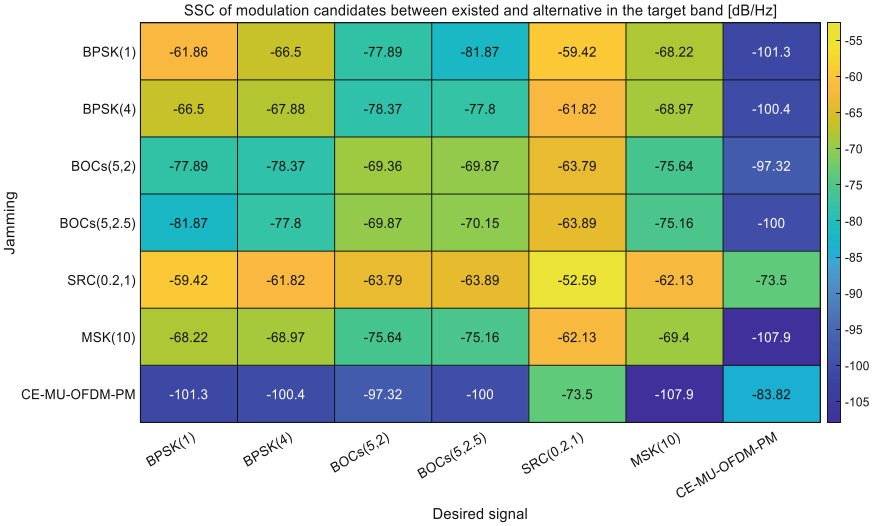


Fig. 7. SSC for proposed and others signal

shows that when CE-MU-OFDM-PM is used as the target signal, other signals have significantly less impact on it as interference signals, while CE-MU-OFDM-PM is used as the interference signal, has a significant impact on the target signals listed in this article is also tiny.

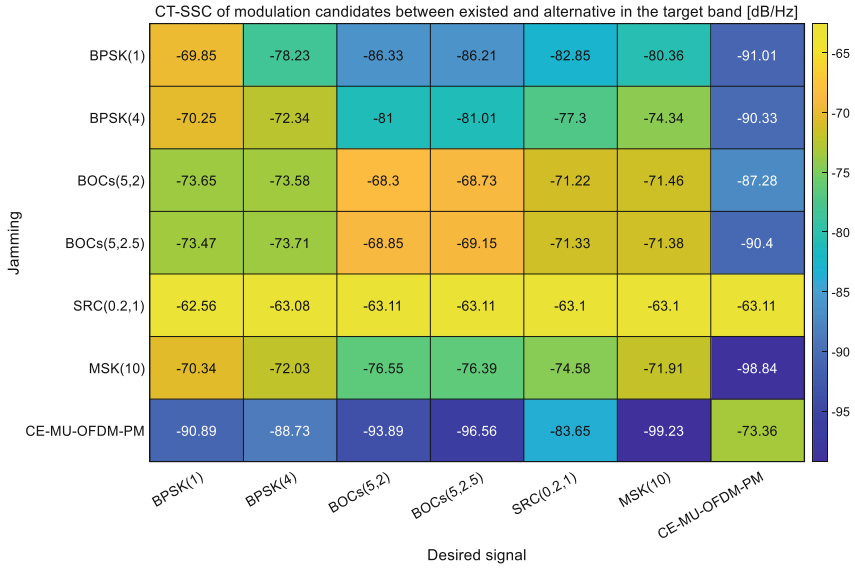


Fig. 8. CT-SSC for proposed and others signal

The above results show that the proposed signal is far more compatible than other candidate signals, has outstanding peeling ability from existing signals, and has very little impact on tracking performance.

Anti-multipath

In this paper, the multipath error envelope and the average multipath error envelope are used as measurement indicators in the anti-multipath capability. The simulation results are shown in Fig. 9 and Fig. 3.

In Fig. 9, it shows the multipath error envelopes of different spread spectrum modulated signals when the multipath delay is within 3000 m. Obviously, the multipath error of CE-MU-OFDM-PM marked by the red dashed line is significantly smaller than other types of spread spectrum modulated signals mean that under the condition of multipath delay within 3000 m, the signal itself has the characteristics of multipath suppression.

In Fig. 10, it shows the average envelope of various spread spectrum modulated signals within 3000 m. The average multipath error of the proposed scheme is within 0.1 m, and this evaluation result far exceeds any other candidate signals listed in this paper. From a statistical point of view, it has excellent line-of-sight propagation and multi-path suppression in different multipath delays.

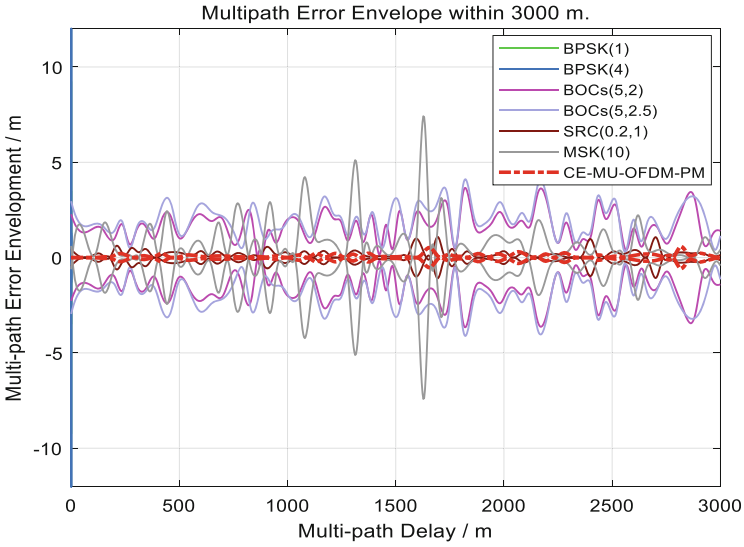


Fig. 9. Multipath capabilities between proposed and others

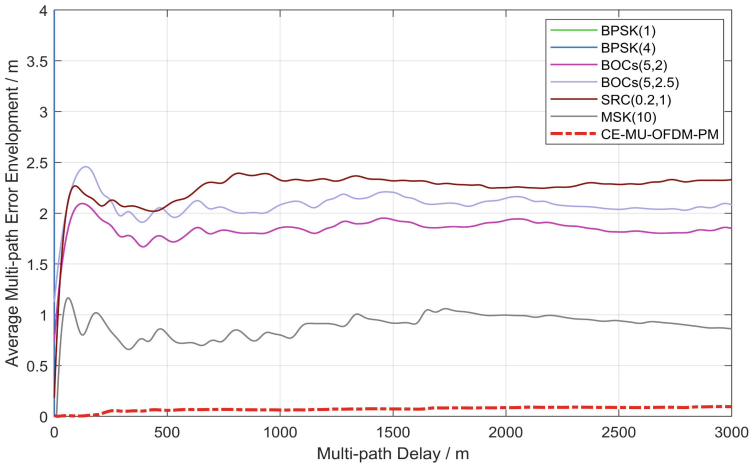


Fig. 10. Average multipath between proposed and others

Anti-Jamming

Anti-jamming capability focuses on anti-matching jamming and anti-narrowband jamming, and on the tracking and demodulation phase. The quality of merit histogram of the anti-jamming is shown in Fig. 11.

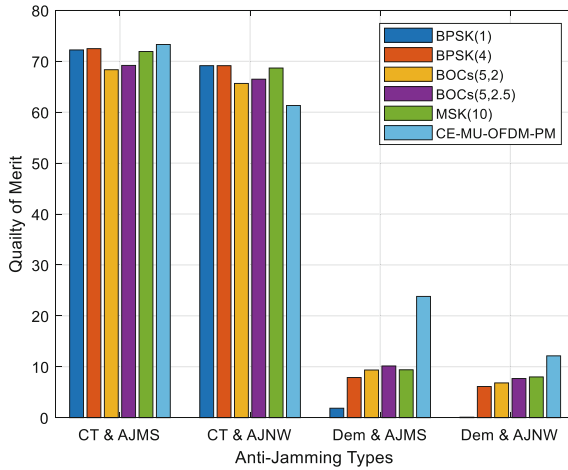


Fig. 11. Anti-jamming for proposed and others

The CE-MU-OFDM-PM signal identified by the blue rectangle bar plays other broadcast signals in the anti-matching spectrum interference performance of the demodulation, while the spread spectrum code tracking anti-interference interference and the anti-narrowband interference performance of the demodulation is similar to other signals. In the spread spectrum code to find out the narrow-band jamming performance is slightly resistant to other signals. It has good anti-interference ability, and can also identify interference to narrow-band jamming and has a good anti-jamming ability.

Spectrum Multiplex

Parameter of CE-MU-OFDM-PM setting to 64, that is, the proposed scheme contains the multiplexing of 64 sub-carriers, and compares it with the normalized power spectral density function of the NSCC (19), as shown in Fig. 12.

In Fig. 12, the proposed scheme and NSCC (19) have larger main lobe bandwidths on the normalized power spectral density, and are more concentrated on a certain carrier frequency offset. At the same time, both have the same excellent main lobe side. The lobe amplitude ratio (PSR) produces a pulse-like pattern within a certain frequency range in the normalized PSD. From the comparison of the signal's own amplitude, the level of NSCC is 5dBW/Hz higher than the proposed signal. It shows that on the low-orbit satellite transmitter in the same bandwidth and antenna gain, NSCC (19) is higher transmission power than CE-MU-OFDM-PM (64). This means that the proposed signal scheme has higher spectrum multiplexing capabilities and higher spectrum efficiency than NSCC, allowing more users to implement spectrum multiplexing on it.

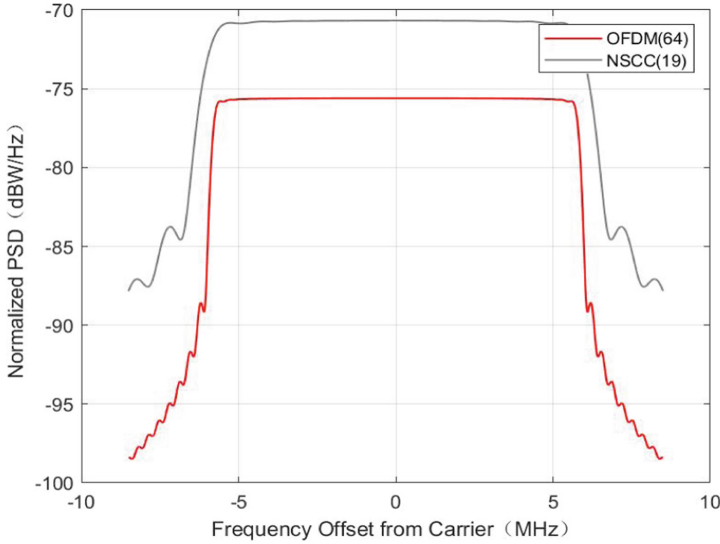


Fig. 12. Proposed signal NPSD compare with NSCC (19)

Communication Link Payload

This paper uses the terms bit signal-to-noise ratio (E_b/N_0) and bit error rate (BER) as indicators in the estimation of communication links.

For the uplink, its bit-to-signal ratio can be expressed as,

$$\begin{aligned}
 E_b/N_0 &= EIRP - (L_0 + L_s) + (G_r/T)_{dB} - (k)_{dB} - 10 \cdot \log(R_b) \\
 &= (11 + 3) - L_0 - 1 - 6.5 + 228.6 - 10 \cdot \log(64000) \\
 &= 187.04 - L_0 \\
 &= 187.04 - [161.21 \sim 167.23]_{dB} \\
 &= [19.81 \sim 25.83]_{dB}
 \end{aligned}$$

For the downlink, its bit-to-signal ratio can be expressed as,

$$\begin{aligned}
 E_b/N_0 &= EIRP - (L_0 + L_s) + (G_r/T)_{dB} - (k)_{dB} - 10 \cdot \log(R_b) \\
 &= (20 + 13) - L_0 - 1 - 13 + 228.6 - 10 \cdot \log(4096000) \\
 &= 19 - L_0 + 228.6 - 66.12 \\
 &= 181.48 - [161.21 \sim 167.23]_{dB} \\
 &= [14.25 \sim 20.27]_{dB}
 \end{aligned}$$

The redundancy of E_b/N_0 in the communication uplink and downlink is 18.4299 dB–29.2671 dB and 13.072 dB–23.8268 dB, respectively. At the same time, even in the worst case, the BER of the uplink can reach $1.0e^{-30}$, and the BER of the downlink is $9.47e^{-11}$, they are significantly better than the $1.0e^{-6}$ threshold.

Based on the above, from a theoretical level, compared with other signals, CE-MU-OFDM-PM has excellent performance like accuracy potential, compatibility, anti-multipath ability, anti-interference ability, spectrum multiplexing ability, and communication link overhead.

The redundancy of E_b/N_0 in the communication uplink and downlink is 18.4299 dB–29.2671 dB and 13.072 dB–23.8268 dB, respectively. At the same time, even in the worst case, the BER of the uplink can reach $1.0e^{-30}$, and the BER of the downlink is $9.47e^{-11}$, they are significantly better than the $1.0e^{-6}$ threshold.

Based on the above, from a theoretical level, compared with other signals, CE-MU-OFDM-PM has excellent performance like accuracy potential, compatibility, anti-multipath ability, anti-interference ability, spectrum multiplexing ability, and communication link overhead.

5 Conclusion and Outlook

This paper proposes a novel CE-MU-OFDM-PM signal modulation method, which not only inherits the characteristics of phase modulation, but also inherits the advantages of orthogonal frequency division multiplexing, and can be implemented in the uplink and downlink design of the communication link. The requirements of E_b/N_0 and BER are verified by the simulation to meet the design requirements of NavCom.

In the point of view of value, CE-MU-OFDM-PM can be used as a potential signal source for NavCom. It can provide a basis for engineering verification on LEOs payloads and even space-based payloads, and provide BDS with a competitive potential signal solution in the future. It can provide a research theoretical basis for the development of portable PNTC terminals in the future.

Acknowledgments. This work is supported by Technological Innovation Project (Major Program) of Hubei Province under Grant 2019AAA025 and National Key R&D Program of China under Grant SQ2021YFB3900243.

References

1. Yuanxi, Y., et al.: Featured services and performance of BDS-3. *Sci. Bull.* **66**(20), 2135–2143 (2021)
2. Liu, J., et al.: Development and trends of marine space-time frame network. *Geomatics Inf. Sci. Wuhan Univ.* **44**(1), 17–37 (2019)
3. Liu, J., et al.: Role, path, and vision of “5G + BDS/GNSS.” *Satell. Navig.* **1**(1), 1–8 (2020)
4. Yang, Y., et al.: PNT intelligent services. *Acta Geodaetica et Cartographica Sinica* **50**(8), 1006–1012 (2021)
5. Li, D., et al.: On civil-military integrated space-based real-time information service system. *Geomatics Inf. Sci. Wuhan Univ.* **42**(11), 1501–1505 (2017)
6. Zhang, F., et al.: Study of PNT architecture-synergy of PNT and communications. *GNSS World China* **39**(001), 19–22 (2014)
7. Deng, Z., Yu, Y., Yuan, X., Wan, N., Yang, L.: Situation and development tendency of indoor positioning. *China Commun.* **10**(3), 42–55 (2013)

8. Liu, X., Liang, M., Morton, Y., Closas, P., Zhang, T., Hong, Z.: Performance evaluation of MSK and OFDM modulations for future GNSS signals. *GPS Solutions* **18**(2), 163–175 (2014). <https://doi.org/10.1007/s10291-014-0368-6>
9. Luo, R., Xu, Y., Hong, Y.: Performance evaluation of the new compound-carrier-modulated signal for future navigation signals. *Sensors* **16**(2), 142 (2016)
10. Cai, C., Luo, X., Liu, Z., Xiao, Q.: Galileo signal and positioning performance analysis based on four IOV satellites. *J. Navig.* **67**(5), 810–824 (2014)
11. Sun, Y.: Optimal parameter design of continuous phase modulation for future GNSS signals. *IEEE Access* **9**, 58487–58502 (2021)
12. Prochniewicz, D., Grzymala, M.: Analysis of the impact of multipath on Galileo system measurements. *Remote Sens.* **13**(12), 2295 (2021)
13. Sun, Y., Xue, R., Zhao, D., Wang, D.: Radio frequency compatibility evaluation of S band navigation signals for future BeiDou. *Sensors* **17**(5), 1039 (2017)
14. Wang, L., Huang, X., Li, J., Tang, X., Wang, F.: Proposal of spread spectrum MSK for BDS RDSS signal modulation. *IET Radar Sonar Navig.* **14**(6), 870–878 (2020)
15. Ji, J., et al.: A SRC-like signal design and performance analysis in S band. In: 16th Proceedings on IAIN World Congress, Chiba, Japan, pp. 1–7 (2018)
16. Darwish, T., et al.: LEO satellites in 5G and beyond networks: a review from a standardization perspective. arXiv preprint: 2110.08654 (2021)